Ferromagnetic insulating and spin glass behavior in Cr substituted $La_{0.85}Ag_{0.15}MnO_3$ compounds

2008 J. Phys.: Condens. Matter 20 235201

(http://iopscience.iop.org/0953-8984/20/23/235201)

J. Phys.: Condens. Matter **20** (2008) 235201 (7pp) doi:10.1088/0953-8984/20/23/235201

Ferromagnetic insulating and spin glass behavior in Cr substituted $La_{0.85}Ag_{0.15}MnO_3$ compounds

S K Srivastava[1], Manoranjan Kar[2] and S Ravi[1]

[1] Department of Physics, Indian Institute of Technology Guwahati, Guwahati-781039, India
[2] Centre for Nanotechnology, Indian Institute of Technology Guwahati, Guwahati-781039, India

E-mail: sravi@iitg.ernet.in

Received 31 January 2008, in final form 4 April 2008
Published 30 April 2008
Online at stacks.iop.org/JPhysCM/20/235201

Abstract

Single phase samples of polycrystalline $La_{0.85}Ag_{0.15}Mn_{1-y}Cr_yO_3$ ($y = 0$, 0.05, 0.10, 0.15, 0.20) were prepared by the solid-state route. These samples were studied by recording x-ray diffraction patterns to investigate their crystal structure, by measuring temperature and frequency variations of ac susceptibility and high temperature magnetization to investigate their magnetic properties and by measuring magneto-resistivity. X-ray diffraction patterns could be refined by using the $R\bar{3}c$ space group. The lattice parameters and Mn–O bond lengths were found to decrease with Cr doping. Paramagnetic to ferromagnetic transitions followed by low temperature spin glass like behavior have been observed from ac susceptibility results. The above transitions could be understood on the basis of double exchange ferromagnetic interaction in Mn^{3+}–O^{2-}–Mn^{4+}, super-exchange ferromagnetic interaction in Cr^{3+}–O^{2-}–Mn^{3+} and super-exchange antiferromagnetic interaction in Mn^{4+}–O^{2-}–Mn^{4+} networks. Even though a strong ferromagnetic signal was observed in all the Cr doped samples, no metal–insulator transition has been observed. Thus Cr doping gives rise to a ferromagnetic insulating state and the Cr might take part in super-exchange ferromagnetic interactions. Colossal magneto-resistivity has been observed up to 20% of Cr doping in a wide temperature range down to low temperatures.

1. Introduction

Mixed valent manganites are the subject of research interest due to their rich variety of physical and chemical properties and potential applications in technologies such as magnetic recording, magnetic actuators, magnetic sensors etc [1–3]. The most interesting property of these materials is colossal magneto-resistivity (CMR) behavior in the vicinity of the paramagnetic to ferromagnetic transition temperature (T_c). Mixed valent manganites with CMR behavior have been observed by doping either divalent alkaline earth elements (Ca, Sr, Ba etc) or mono-valent alkali ions (K, Na, Ag etc) in place of the rare earth element R in $RMnO_3$ [1–6]. The CMR behavior can be explained qualitatively by using Zener double exchange (DE) ferromagnetic interaction in Mn–O–Mn networks [7]. In addition to DE interactions, other mechanisms such as super-exchange interactions, electron–phonon interactions, spin fluctuations, electron magnon interactions etc have to be taken into account to explain the rich physical and chemical properties of these manganites [8]. The effect of Mn site doping using other transition elements, such as T = Ti, Cu, Cr, Fe, Co, Ni, Ru and non-magnetic element Al have been studied by several groups [9–23]. It is found that Mn site doping generally gives rise to a decrease in Curie temperature and metal–insulator (M–I) transition temperature.

Among the 3d transition elements, Cr substitution is particularly interesting, as Cr^{3+} is iso-electronic with Mn^{4+} and the non-Jahn–Teller ion. Paramagnetic (PM) to ferromagnetic (FM) transition has been reported in the Cr substituted parent compound $LaMn_{1-x}Cr_xO_3$ [15]. Reentrant spin glass behavior has been reported in $La_{0.46}Sr_{0.54}Mn_{1-y}Cr_yO_3$ for $y = 0.02$ [24]. Wu *et al* [18] have observed that doping of Cr ions dilutes the long range ferromagnetic ordering of $La_{0.7}Ca_{0.3}Mn0_3$. They have observed the Kondo effect and

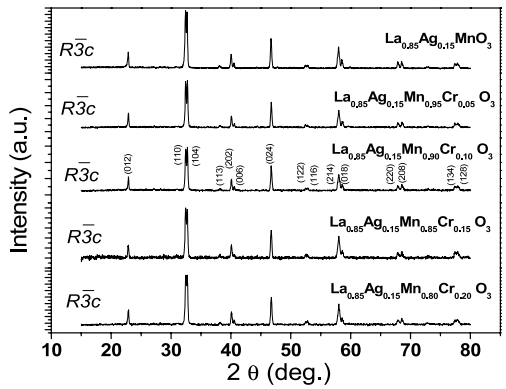

Figure 1. XRD patterns of the samples $La_{0.85}Ag_{0.15}Mn_{1-y}Cr_yO_3$ ($y = 0$, 0.05, 0.10, 0.15 and 0.20).

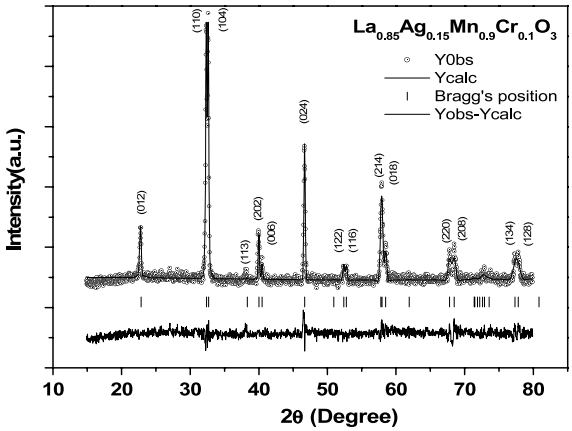

Figure 2. XRD pattern for the sample y = 0.10. The circles represent experimental points and the solid line represents Rietveld refined data. The bottom line shows the difference between experimental and refined data. The marked 2θ positions are the allowed Bragg peaks.

spin glass behavior for $La_{0.7}Ca_{0.3}Mn_{1-x}Cr_x0_3$ ($x = 0.05$, 0.1 and 0.3). An increase in T_c and spin glass behavior has been observed in $La_{0.9}Ca_{0.1}Mn_{1-y}Cr_yO_3$ ($y = 0.01$ and 0.2) samples [19]. Ganguly *et al* [11] have considered ferromagnetic super-exchange interaction in Mn^{3+}–O^{2-}–Cr^{4+} networks to explain the magnetic behavior of $La_{0.7}Ca_{0.3}Mn_{1-x}Cr_xO_3$. The interaction between Cr–Mn ions in manganites is yet to be understood in detail.

In this report, we have chosen mono-valent doped double exchange ferromagnetic $La_{0.85}Ag_{0.15}MnO_3$ to substitute Cr in the Mn site. We have observed a spin glass like transition at low temperature in addition to FM and antiferromagnetic (AFM) transitions. The magnetic property of the present series of samples is explained on the basis of the super-exchange ferromagnetic interaction in Cr–O–Mn networks. The rate of fall of ferromagnetic T_c with Cr concentration is found to be small compared to other transition element doping, such as Fe and Co.

2. Experimental details

Polycrystalline samples of the $La_{0.85}Ag_{0.15}Mn_{1-y}Cr_yO_3$ series for $y = 0$, 0.05, 0.10, 0.15, 0.20 were prepared by the conventional solid-state reaction method. Stoichiometric ratio of La_2O_3, $AgNO_3$, Mn metal powder and CrO_3 with 99.9% purity were weighed and mixed thoroughly under acetone. The mixture was presintered at 300, 400, 500, 600 and 700 °C for 5 h at each temperature and at 800 °C for 36 h with intermediate grindings. The sintering in pellet form was carried out for 36 h at 1000 °C and 1100 °C respectively with a few intermediate grindings. All the above sintering was carried out in atmospheric pressure. X-ray diffraction (XRD) patterns were recorded at room temperature using a Bruker D8 Advance XRD machine with Cu Kα radiation. Scanning electron micrographs were taken by using a LEO scanning electron microscope (SEM). Compositional analysis has been carried out by recording the energy dispersive spectrum using the Oxford energy dispersive spectrometer (EDS) attached to the SEM. Temperature variation of ac susceptibility down to 30 K was measured by the mutual inductance bridge method. The frequency variation of ac susceptibility was carried out at five different frequencies, namely 333, 1333, 3333, 6333 and 9333 Hz in an applied field of 2 Oe. A temperature variation of DC magnetization was measured from room temperature to 500 K using a Lake Shore Vibrating Sample Magnetometer (VSM). DC electrical resistivity as a function of temperature was measured down to 30 K by employing the linear four probe technique. The magneto-resistivity was measured by applying a magnetic field of 10 kOe. A commercial closed cycle helium refrigerator cryostat equipped with a temperature controller was used for temperature variations down to 30 K.

3. Results and discussions

3.1. Crystal structure

The XRD patterns recorded for $La_{0.85}Ag_{0.15}Mn_{1-y}Cr_yO_3$ compounds with $y = 0$, 0.05, 0.10, 0.15 and 0.20 are shown in figure 1. We can see that the samples are in single phase form. The XRD patterns were analyzed with the help of the Fullprof program by the Rietveld refinement technique [25]. The patterns for all the samples could be refined using the $R\bar{3}c$ space group; they were consistent with those reported for $La_{0.85}Ag_{0.15}MnO_3$ [26, 27]. Typical XRD patterns along with Rietveld refinement are shown in figure 2 for $y = 0.10$. Here the experimental data are shown as circles and calculated intensities are shown as solid lines. The bottom lines represent the difference between measured and calculated intensities. The allowed Braggs positions for the $R\bar{3}c$ space group are marked as small vertical lines. One can see that all the observed peaks coincide with the allowed Bragg 2θ positions.

The refined lattice parameters and unit cell volume are listed in table 1. These values are comparable to those reported for $La_{1-x}Ag_xMnO_3$ [26, 27]. The lattice parameters and unit cell volume are found to decrease with Cr doping. The average Mn–O bond length and ∠ Mn–O–Mn bond angle are calculated from the refined atomic positions and lattice parameters and these values are tabulated in table 1. Bond angles Mn–O–Mn are found to increase with increase in Cr concentration. The average bond distance Mn–O decreases with Cr doping.

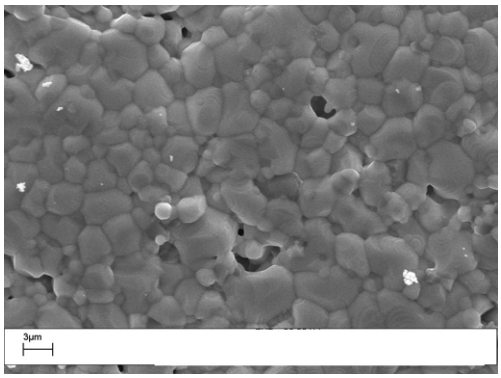

Figure 3. SEM image (magnification 8000) of the $La_{0.85}Ag_{0.15}Mn_{0.85}Cr_{0.15}O_3$ sample.

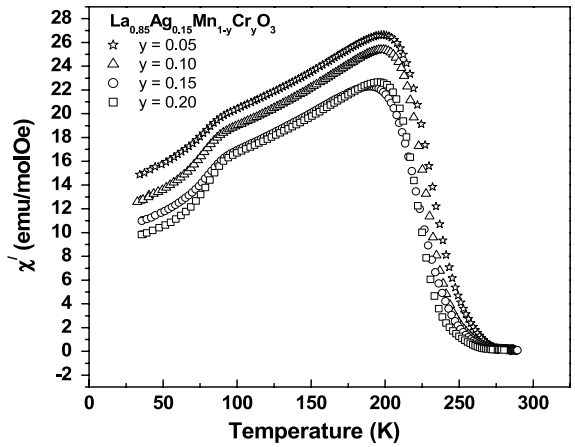

Figure 4. Temperature variation of in-phase ac susceptibility (χ') of samples $La_{0.85}Ag_{0.15}Mn_{1-y}Cr_yO_3$ ($y = 0.05$, 0.10, 0.15 and 0.20).

Table 1. Parameters obtained from the Rietveld analysis of XRD patterns for the samples $La_{0.85}Ag_{0.15}Mn_{1-y}Co_yO_3$ ($y = 0.05$, 0.10, 0.15 and 0.20). Errors of lattice parameters and unit cell volume are shown in brackets.

	Sample			
Parameters	$y = 0.05$	$y = 0.10$	$y = 0.15$	$y = 0.20$
Space group	$R\bar{3}c$	$R\bar{3}c$	$R\bar{3}c$	$R\bar{3}c$
$a = b$ (Å)	5.5318 (0.0013)	5.5306 (0.0014)	5.5265 (0.0019)	5.52780 (0.0014)
c (Å)	13.3772 (0.0034)	13.3763 (0.0037)	13.3715 (0.0050)	13.3826 (0.0036)
Volume (Å^3)	354.5 (0.1)	354.3 (0.2)	353.7 (0.2)	354.2 (0.2)
χ^2 (%)	2.48	2.28	2.05	2.25
R_p (%)	7.83	8.34	7.74	7.75
Mn–O (Å)	1.970	1.967	1.965	1.964
Mn–O–Mn (deg)	162.5	163.8	163.9	165.1

A typical SEM micrograph for $La_{0.85}Ag_{0.15}Mn_{0.15}Cr_{0.15}O_3$ is shown in figure 3. The morphology of the sample is found to be uniform. The composition determined from EDS analysis is found to be comparable to the nominal starting composition. The EDS analysis shows that the cationic ratio for the $y = 0.15$ sample is La:Ag:Mn:Cr = 0.88:0.12:0.87:0.13.

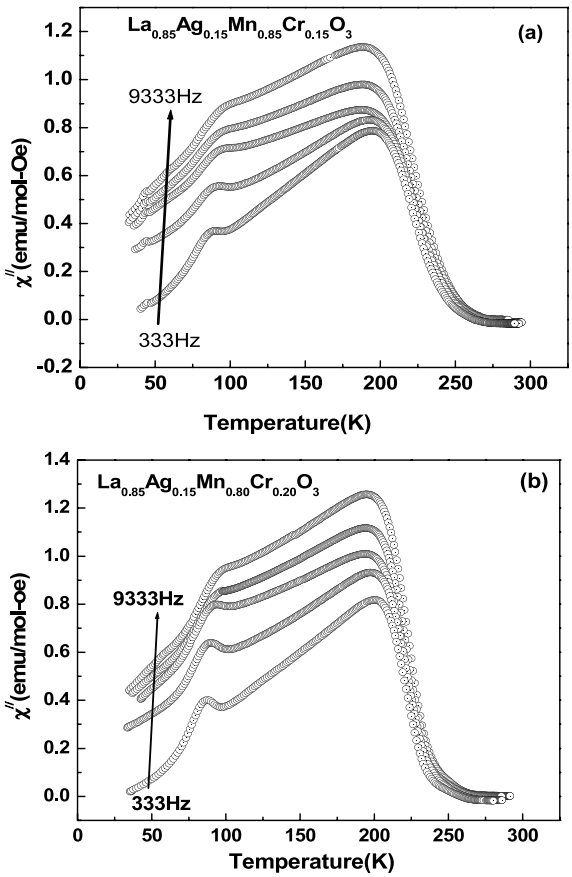

Figure 5. χ'' versus temperature (T) measured at frequencies $f = 333$, 1333, 3333, 6333 and 9333 Hz for the samples (a) $y = 0.15$ and (b) 0.20.

3.2. Ac susceptibility

The temperature variations of χ' are shown in figure 4 for the samples $La_{0.85}Ag_{0.15}Mn_{1-y}Cr_yO_3$ ($y = 0.05$, 0.10, 0.15 and 0.20). All the materials exhibit paramagnetic to ferromagnetic (FM) transition under cooling. The FM transition could be understood due to the double exchange interaction between Mn^{3+}–O^{2-}–Mn^{4+} networks and super-exchange (SE) ferromagnetic interaction in Cr^{3+}–O^{2-}–Mn^{3+} networks. The ferromagnetic transition temperature has been determined from the temperature corresponding to a negative peak in the $d\chi'/dT$ versus T plot. The peak temperature was taken by fitting the curve to a Gaussian function. The T_c is found to be 284 K for $La_{0.85}Ag_{0.15}MnO_3$ and it is comparable to that of the reported value [26, 27]. The values of FM T_c are given in table 2 and they decrease with increase in doping. This could be due to dilution of the strong double exchange ferromagnetic interaction in Mn^{3+}–O^{2-}–Mn^{4+} networks. However, the fall in $T_c(\frac{\Delta T_c}{T_c} \times 100)$ is about 23%, 25%, 27% and 28% for $y = 0.05$, 0.10 0.15 and 0.20, with respect to the $y = 0$ sample, which is quite small compared to Co doped samples [22]. It could be due to the presence of ferromagnetic SE interactions in the Cr^{3+}–O^{2-}–Mn^{3+} network along with DE ferromagnetic interactions in Mn^{3+}–O^{2-}–Mn^{4+} networks.

Temperature variations of magnetization from 300 to 500 K were carried out to determine the variation of the

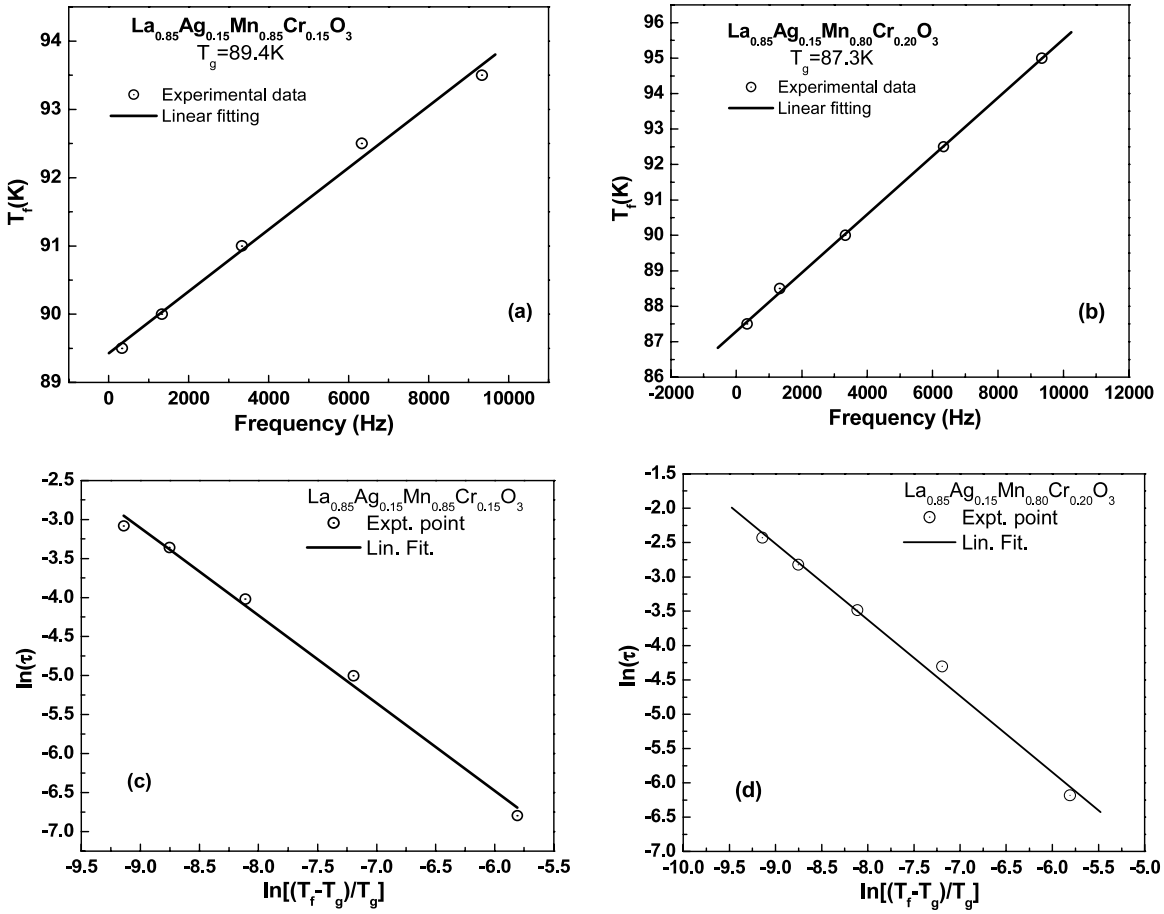

Figure 6. Plots of T_f versus frequency for the samples (a) $La_{0.85}Ag_{0.15}Mn_{0.85}Cr_{0.15}O_3$ and (b) $La_{0.85}Ag_{0.15}Mn_{0.8}Cr_{0.2}O_3$ and the plots of $\ln(\tau)$ versus $\ln[(T_f–T_g)/T_g]$ for (c) $La_{0.85}Ag_{0.15}Mn_{0.85}Cr_{0.15}O_3$ and (d) $La_{0.85}Ag_{0.15}Mn_{0.8}Cr_{0.2}O_3$.

Table 2. Parameters obtained from the linear ac susceptibility of $La_{0.85}Ag_{0.15}Mn_{1-y}Cr_yO_3$. T_{on} and T_c are ferromagnetic onset and transition temperatures respectively. χ'_m is the maximum susceptibility. θ (Curie temperature), C (Curie constant), μ_{eff} (μ_B) are calculated from high temperature magnetization measurement.

Sample	$y = 0.00$	$y = 0.05$	$y = 0.10$	$y = 0.15$	$y = 0.20$
T_{on} (K)	—	280	276	275	270
T_c (K)	284	231	227	224	222
χ'_m (emu mol^{-1} Oe^{-1})	27.94	26.62	25.38	22.29	22.10
θ (K)	301	247	241	237	235
C (K emu mol^{-1} Oe^{-1})	2.98	2.91	2.88	2.86	2.83
μ_{eff} (μ_B)	4.88	4.82	4.79	4.78	4.75

paramagnetic Curie temperature θ, Curie constant C and effective magnetic moment μ_{eff}. The plot of inverse dc susceptibility ($1/\chi_{dc}$) versus temperature (T) exhibits a linear behavior (not shown) in the paramagnetic region. We have fitted the data by using the Curie–Weiss law, $\chi = C/(T - \theta)$ and the values of C, θ and μ_{eff} are given in table 2. One can see that θ is positive as expected for paramagnetic to ferromagnetic transition behavior. θ is found to decrease with increase in Cr concentration, which reflects the decrease in double exchange FM interaction and it is in correlation with the variation of FM T_c with doping. Even though θ and T_c follow the same trend with doping, the θ value is found to be higher than that of T_c for each sample. This could be mainly due to smearing of the FM transition as a result of different types of FM interaction or dilution of the DE FM interaction.

All the Cr doped samples exhibit a low temperature fall in susceptibility at around 90 K along with the corresponding peak in the χ'' versus T plot (figure 5). They can be attributed to a spin glass like transition. This could be due to the presence of competing antiferromagnetic interaction in the Mn^{4+}–O^{2-}–Mn^{4+} network and different types of ferromagnetic interactions in Mn^{3+}–O^{2-}–Mn^{4+} and Cr^{3+}–O^{2-}–Mn^{3+} networks.

To understand the origin of the low temperature peak observed in the χ'' versus temperature plot (figure 5), we have carried out the temperature variations of ac susceptibility at different frequencies such as, 333, 1133, 3333, 6333

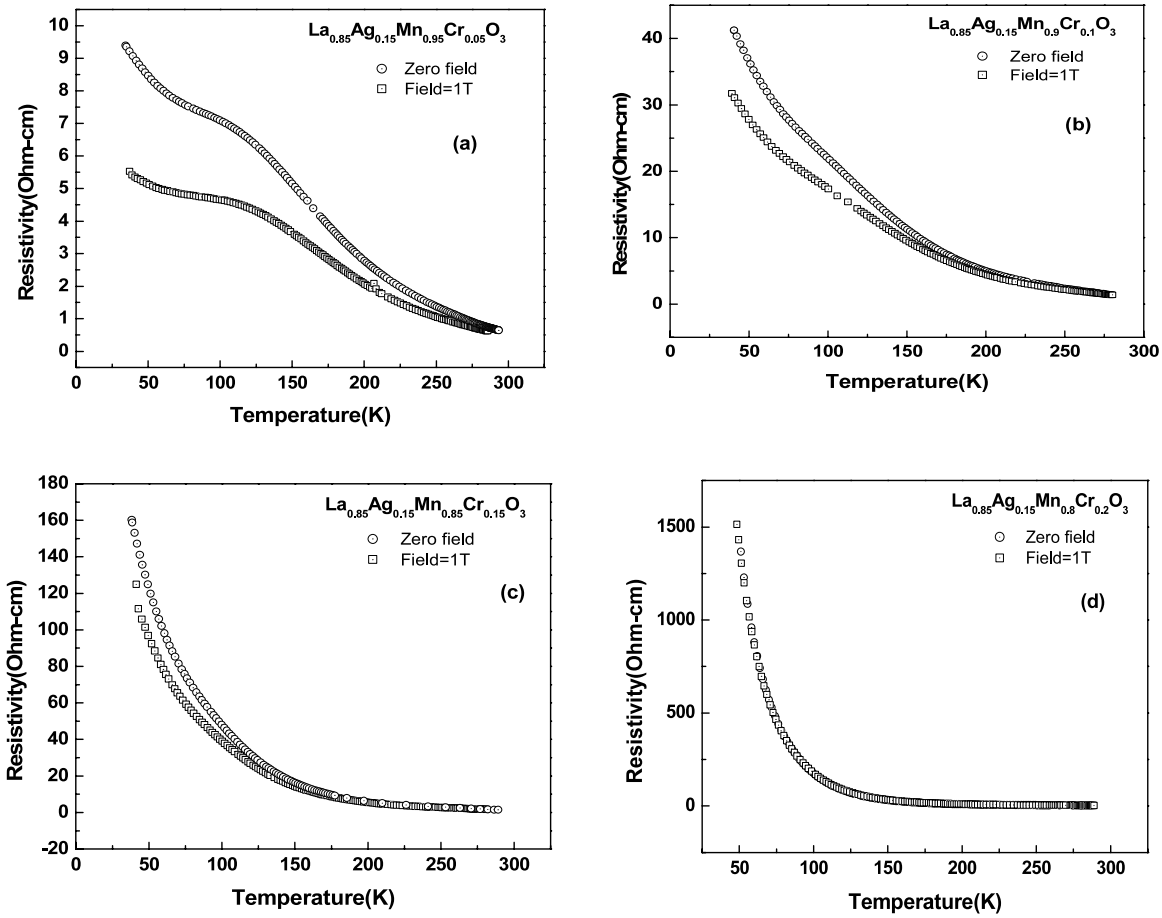

Figure 7. Temperature variation of electrical resistivity and magneto-resistivity of $y = 0.05$, 0.10, 0.15 and 0.20 samples.

and 9333 Hz. Typical plots of χ'' versus temperature for different frequencies are shown in figure 5 for $y = 0.15$ and 0.20 samples. We have not found any change in the position of the ferromagnetic transition temperature T_c with frequency. However, low temperature peak shifts towards higher temperature with increase in frequency. These features are commonly observed in conventional spin glass systems. The temperature corresponding to the above peak is taken as the spin glass freezing temperature T_f.

We have analyzed the spin glass like transition at low temperature from the frequency dependent data based on the power law relation [28],

$$\frac{\tau}{\tau_0} = \left[\frac{T_f - T_g}{T_g}\right]^{-Z\nu}. \qquad (1)$$

Here, τ is the relaxation time corresponding to the measured frequency ($\tau = 1/f$), τ_0 is the characteristic time constant and $z\nu$ is the critical exponent. T_g is the spin glass transition temperature, which is equivalent to the freezing temperature in the limit of $\tau \to \infty$, i.e. $f \to 0$. A typical plot of T_f versus frequency is shown in figures 6(a) and (b), for the samples $y = 0.15$ and 0.20 respectively. These data were fitted to the linear equation to determine T_g and the fitted data are shown as solid lines. A typical plot of $\ln(\tau)$ versus $\ln[(T_f - T_g)/T_g]$ is shown in figures 6(c) and (d) for the samples $y = 0.15$ and 0.20. These data were fitted to equation (1) by varying the parameters τ_0 and $z\nu$ and the fitted data are shown as a solid line. The typical τ_0 and $z\nu$ values are listed in table 3 for all samples. The τ_0 is much higher than the value observed in a conventional spin glass system (10^{-13} s) [29].

3.3. Resistivity and magneto-resistivity

The temperature variations of electrical resistivity (ρ) in the absence and presence of 10 kOe magnetic field are shown in the figure 7 for samples $La_{0.85}Ag_{0.15}Mn_{1-y}Cr_yO_3$ ($y = 0.05$, 0.10, 0.15 and 0.20). A broad hump has been observed at around 120 and 100 K for $y = 0.05$ and 0.10 samples respectively. The broad hump indicates that metallic behavior competes with insulating behavior and the system re-enters into an insulating state. Semiconducting behavior has been observed for $y \geqslant 0.15$ samples. Even though the Cr doped samples exhibit an FM transition with strong FM signal, we have not observed a clear metal–insulator transition. This can be attributed to the domination of super-exchange FM interaction in Cr^{3+}–O^{2-}–Mn^{3+} networks with increase in Cr doping. Thus Cr doping leads to the ferromagnetic insulating state.

The temperature variation of magneto-resistivity was calculated using the relation, $(\Delta\rho/\rho_o) = (\rho_H - \rho_o)/\rho_o$. Here ρ_H is the resistivity in the presence of magnetic field and ρ_0 is the resistivity in the absence of magnetic field at a given

Table 3. Parameters obtained from the frequency variation of ac susceptibility measurements. T_f and T_g are the spin glass freezing temperature and spin glass temperature respectively. τ_0 is the characteristic time constant.

Sample		$y = 0.00$	$y = 0.05$	$y = 0.10$	$y = 0.15$	$y = 0.20$
T_f (K)	333 Hz		84.5	86.5	89.5	87.5
	1333 Hz		85.5	87.0	90.0	88.5
	3333 Hz	—	87.0	88.5	91.0	90.0
	6333 Hz		89.0	90.5	92.5	92.5
	9333 Hz		91.0	92.0	93.5	95.0
T_g (K)		—	84.4	86.3	89.4	87.3
τ_0 (10^{-6} s)		—	1.659	5.516	1.830	3.700
$z\nu$		—	1.194	1.032	1.122	1.109

temperature. The temperature variation of negative magneto-resistivity ($-\Delta\rho/\rho_0$) is shown in figure 8 for $y = 0.05$ and 0.10 samples. Broad magneto-resistivity peaks have been observed at around 240 K for $y = 0.05$ sample, 230 K for $y = 0.10$ and 225 K for $y = 0.15$ samples and they are comparable to the FM T_c observed from ac susceptibility measurements. Thus the electrical resistivity and magneto-resistivity data show that in Cr doped samples there is a contribution from both metallic conduction due to double exchange ferromagnetic interaction and semiconducting behavior due to ferromagnetic/antiferromagnetic super-exchange interaction. Unlike the conventional CMR materials where large magneto-resistivity (MR) is observed only in the vicinity of FM T_c, here we can observe considerable MR in a wide temperature range. The increase in MR with decrease in temperature can be explained on the basis of the presence of considerable magnetic anisotropy and it is suppressed due to applied magnetic field. The contribution of intergranular tunneling can be also one of the reasons for the observed MR.

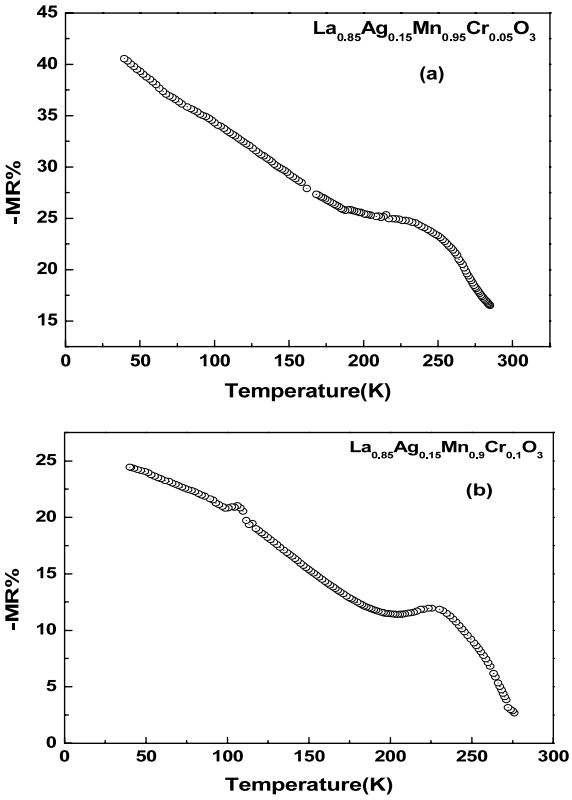

Figure 8. Temperature variation of MR ($-\Delta\rho/\rho_0$) for the samples (a) $La_{0.85}Ag_{0.15}Mn_{0.95}Cr_{0.05}O_3$ and (b) $La_{0.85}Ag_{0.15}Mn_{0.90}Cr_{0.10}O_3$.

4. Conclusions

$La_{0.85}Ag_{0.15}Mn_{1-y}Cr_yO_3$ compounds have been prepared for $y = 0$–0.20. All the samples are found to be in single phase form. The Rietveld analysis of XRD patterns shows that the observed peak could be indexed to the $R\bar{3}c$ space group. Paramagnetic to ferromagnetic transitions followed by low temperature spin glass like transitions have been observed for Cr doped samples. Unlike the other magnetic element doping, the rate of decrease in T_c with doping and reduction in susceptibility magnitude are quite small in Cr doped materials. On the other hand, there is a large change in resistivity behavior due to Cr doping and the signature of competing metallic behavior with insulating behavior was observed up to 10% of Cr doping. The above observation suggests that the role of Cr is to dilute the DE FM interaction and possible super-exchange interactions in the Cr^{3+}–O^{2-}–Mn^{3+} network. The Cr ions are expected to replace the Mn^{3+} ions and hence encourage antiferromagnetic super-exchange interaction in Mn^{4+}–O^{2-}–Mn^{4+} networks. These competing magnetic interactions also give rise to low temperature spin glass like behavior, as confirmed from the frequency variation of ac susceptibility. The spin glass transition temperature is found to increase with doping. The Curie temperature determined from high temperature magnetization measurement is found to be in correlation with FM T_c. The observed CMR in a wide temperature range is explained on the basis of magnetic anisotropy and intergranular tunneling.

Acknowledgment

The authors are thankful to the Department of Science and Technology (DST), New Delhi, India for financial support towards a magnetic measurement system.

References

[1] Rao C N R and Raveau B 1998 *Colossal Magneto Resistance, Charge Ordering and Related Properties of Manganese Oxides* (Singapore: World Scientific)
[2] Tokura Y 2000 *Colossal Magneto-Resistive Oxides* (London: Gordon and Breach)

[3] Nagaev E L 2001 *Phys. Rep.* **346** 387
[4] Boudaya C, Laroussi L, Dhahri E, Joubert J C and Cheikh-Rouhou A 1998 *J. Phys.: Condens. Matter* **10** 7485
[5] Roy S, Guo Y Q, Venkatesh S and Ali N 2001 *J. Phys.: Condens. Matter* **13** 9547
[6] Kar M and Ravi S 2004 *Mater. Sci. Eng.* B **107** 332
[7] Zener C 1951 *Phys. Rev.* **81** 440
[8] Dagotto E, Hotta T and Moreo A 2001 *Phys. Rep.* **344** 1
[9] Gayatri N, Raychaudhuri A K, Tiwary S K, Gundakaram R, Arulraj A and Rao C N R 1997 *Phys. Rev.* B **56** 1345
[10] Rubinstein M, Gillespie D J, Snyder J E and Tritt T M 1997 *Phys. Rev.* B **56** 5412
[11] Ganguly R, Gopalakrishnan I K and Yakhmi J V 1999 *Physica* B **266** 332
[12] Fan X J, Zhang J H, Li X G, Wu W B, Wan J Y, Lee T J and Ku H C 1999 *J. Phys.: Condens. Matter* **11** 3141
[13] Tai M F, Lee F Y and Shi J B 2000 *J. Magn. Magn. Mater.* **209** 148
[14] Gundakaram R, Arulraj A, Vanitha P V, Rao C N R, Gayathri N, Raychaudhuri A K and Cheetham A K 1996 *J. Solid State Chem.* **127** 354
[15] Ahn K H, Wu X W, Liu K and Chien C L 1996 *Phys. Rev.* B **54** 15299
[16] Sahana M, Satyalakshmi K M, Hegde M S, Prasad V and Subramanyam S V 1997 *Mater. Res. Bull.* **32** 831
[17] Ranjan S K and Sundar M S 2003 *Solid State Sci.* **5** 549
[18] Wu B M, Li B, Zhen W H, Ausloos M, Du Y L, Fagnard J F and Vanderbemden Ph 2005 *J. Appl. Phys.* **97** 103908
[19] Sudyoadsuk T, Suryanarayanan R and Winotai P 2005 *Mater. Res. Bull.* **40** 159
[20] Srivastava S K, Kar M and Ravi S 2008 *Mater. Sci. Eng.* B **147** 84
[21] Srivastava S K, Kar M and Ravi S 2006 *J. Magn. Magn. Mater.* **307** 318
[22] Srivastava S K, Kar M and Ravi S 2008 *J. Magn. Magn. Mater.* at press
[23] Cai J W, Wang C, Shen B G, Zhao J G and Zhan W S 1997 *Appl. Phys. Lett.* **71** 1727
[24] Dho J, Kim W S and Hur N H 2002 *Phy. Rev. Lett.* **89** 027202
[25] Young R A 1996 *The Rietveld Method International Union of Crystallography* (New York: Oxford University Press)
[26] Pi L, Hervieu M, Maignan A, Martin C and Raveau B 2003 *Solid State Commun.* **126** 229
[27] Kar M and Ravi S 2004 *Mater. Sci. Eng.* B **110** 46
[28] Gencer A, Ercan I and Özçelik B 1998 *J. Phys.: Condens. Matter* **10** 191
[29] Chikazawa S, Matsuyama H, Sandberg C J and Miyako Y 1981 *J. Phys. Soc. Japan* **50** 2884